Fine Chemical Engineering
http://ojs.wiserpub.com/index.php/FCE/

Research Article

Green Synthesis of Cu_2O Nanoparticles and Their Application for the Photodegradation of Methyl Orange in Aqueous Media

Phung Khac Nam Ho

Institute of Chemistry and Materials, 17 Hoang Sam, Nghia Do, Cau Giay, Hanoi, Vietnam
Email: homyhu@gmail.com

Received: 9 January 2024; **Revised:** 27 February 2024; **Accepted:** 13 March 2024

Abstract: The existence of colorants in water has caused many disadvantages to aquatic systems and the environment. Scientists have made efforts to decompose and remove them using many different methods. In this study, Cu_2O nanoparticles were synthesized with a mixture of reducing agents, including glucose and ascorbic acid, as a photocatalyst for decomposing azo dyes. The prepared nano Cu_2O was fully characterized using scanning electron microscope (SEM) imaging, X-ray diffraction (XRD) diffraction measurements, and band gap energy determination. The obtained nano Cu_2O was of a uniform truncated block shape with particle size ranging from 50 to 150 nm. The prepared nano Cu_2O showed remarkable photocatalytic behavior toward methyl orange under visible light radiation with the removal percentage of 95.46% after 4 hours of reaction. In addition, the catalyst can be reused many times without much impact on catalytic efficiency. Photocatalytic degradation using Cu_2O nanoparticles is a promising method for the removal of methyl orange, contributing to creating a safe and sustainable environment.

Keywords: copper(I) oxide, nanoparticle, green chemistry, photocatalysis, methyl orange dye

1. Introduction

Colorants called azo dyes have one or more azo groups (-N = N-), primarily employed in consumer goods, food, and cosmetics technology.[1,2] Technological applications include laser dyes, photonics, antioxidants, anti-bacterial and anti-cancer drugs.[3-6] In these applications, the textile industry generates large amounts of dye wastewater, which is toxic and non-biodegradable. These dyes cause serious environmental pollution problems due to the release of toxic and carcinogenic substances. The color of these pigments is unsightly and affects soil and aquatic life.[2,7-8] Some industries and factories release waste into the environment without treatment, causing substantial environmental pollution. The demand for colorants is so high that thousands of colorants are produced for use in large quantities around the world. Azo dyes are also known as potential carcinogens. Studies have found that azo dyes resist conventional wastewater treatment processes and do not decompose under natural environmental conditions. Certain azo dyes degrade over time, releasing substances known as aromatic amines, some of which are carcinogenic.[9-10] They are easily absorbed when in contact with the skin, entering the body and causing DNA damage in humans.[11] One of the most critical contaminants is synthetic colorants. Methyl orange (MO) is an acidic azo artificial colorant used in the textile industry and is a known carcinogen that can damage the hematopoietic system due to its substantial toxicity.[11]

Around the world, the problem of treating organic color pollution in surface water and waste water has been

DOI: https://doi.org/10.37256/fce.5120244244

researched, mentioned, and given attention. Removing highly organic pigments from sewage is a very urgent issue. It has great significance in treating clean water for human needs and ensuring water quality and safety for human health. Treating hazardous, non-biodegradable waste is a concern and attracts domestic and international researchers, improving the efficiency of treatment measures and reducing costs. Research into new materials and advanced materials applied to environmental treatment has received and continues to receive special attention from domestic and international scientists. Many methods have been used, such as adsorption,[12-14] electrochemical,[15-17] microorganisms,[18-20] photocatalyst degradation,[21-24] etc., to remove methyl orange.

Cu_2O has a narrow direct band gap energy of 2.0-2.2 eV, making it a p-type semiconductor. Therefore, Cu_2O has an advantage in using sunlight compared to semiconductors with expansive band gap energy, such as TiO_2, ZnO, SnO_2, CdS, $ZnWO_4$, etc. On the other hand, Cu_2O has many beneficial intrinsic properties. Other advantages include low toxicity and environmental friendliness. The primary raw material used is copper, which is widely available in nature, has a low cost, and is a simple, inexpensive material manufacturing process. These advantages make the material Cu_2O have potential applications in various fields: photovoltaics,[25-26] photocatalysts,[27-32] gas sensors,[33-35] high-performance solar cells,[36-38] etc. Cu_2O has been synthesized by several methods, such as hydrothermal,[39] thermal decomposition,[39] wet precipitation[40], electrochemical,[41] etc. The green synthesis pathway of nano Cu_2O has attracted enormous attention from scientists recently.

Herein, Cu_2O nanoparticles are fabricated using a green reducing agent mixture of glucose and ascorbic acid with ethylene glycol. The obtained Cu_2O was evaluated for its characteristics and ability to photocatalyse the decomposition of methyl orange dye.

2. Experimental section

2.1 *Materials*

Copper (II) sulfate pentahydrate (99%, $CuSO_4 \cdot 5H_2O$), Sodium hydroxide (95%, NaOH), Glucose (99%, $C_6H_{12}O_6$), Ascorbic acid (99%, $C_6H_8O_6$), Ethylene glycol ($(CH_2OH)_2$, 99.8%), and Sodium potassium tartrate (99%, $NaKC_4H_4O_6 \cdot 4H_2O$) were purchased from Macklin.

2.2 *Synthesis of Cu_2O nanoparticles*

50 mL of NaOH 2 M + $NaKC_4H_4O_6$ 1.5 M solution was added drop-wise into 50 mL of $CuSO_4$ 0.1 M solution and stirred for 15 minutes. After that, 2 mL of ethylene glycol and 10 mL of ascorbic acid 0.6 M + glucose 0.6 M solution were added to the solution, stirring for an hour at 60 °C. The precipitate was vacuum filtered and thoroughly risen with absolute ethanol and deionized water 2-3 times and dried at 60 °C for 12 hours. The obtained Cu_2O nanoparticles were stored in the vacuum for further characterization.

2.3 *Characterization*

X-ray diffraction with CuKa (λ = 1.5418 Å) was used to describe the crystalline phase of the produced samples, with a scanning rate of 5°/min. The samples' morphology was determined using a scanning electron microscope. An Ultraviolet and visible spectrophotometer (UV-Vis) was used to measure the diffuse reflectance UV-Vis diffuse reflectance spectroscopy (DRS) spectra.

The photocatalytic activity of the prepared Cu_2O nanoparticles: In each typical experiment, 25 mg Cu_2O was exposed to 50 mL of 10 $mg \cdot L^{-1}$ MO solution in a transparent glass tube. The adsorption process took place in the dark after 30 minutes. Then, the glass tubes are put into the lighting cabinet, using the light source as a Xenon lamp (350 W) under air circulation conditions. The MO solution was removed from the mixture after a predetermined amount of time, and the concentration was measured using UV-Vis photometry on UV-Vis DV-8200 equipment (Drawell). The equation to determine MO concentration was built as follows: $C = 14.012 \cdot Abs + 0.2768$ ($R^2 = 0.9983$) where C is the concentration of MO solution, $mg \cdot L^{-1}$; Abs is the light absorption intensity at λ = 464 nm.

The degradation efficiency of MO in the presence of a catalyst is calculated according to the formula:[14]

$$H(\%) = \frac{(C_0 - C_t)}{C_0} \times 100\% \quad (1)$$

The MO removal data by photocatalysis were fed into a pseudo-first-order kinetic model for kinetic analysis:

$$-\ln \frac{C_t}{C_0} = k_1 \times t \quad (2)$$

Where C_0 and C_t are concentrations of MO ($mg \cdot L^{-1}$) initially and at time t, and k_1 is the reaction rate constant.

3. Results and discussion

3.1 *Characterization of the prepared Cu_2O nanoparticles*

The Cu_2O's crystal structure was observed by examining the XRD pattern (Figure 1). The 2θ diffraction peaks at 29.6°, 36.5°, 42.4°, 61.5°, 73.7°, and 77.6°, respectively, are in excellent accord with the standard cards (JCPDS file no. 05-0667) of Cu_2O.[40,42] These correspond to the [110], [111], [200], [220], [311] and [222] crystal planes of Cu_2O. The absence of Cu, CuO, and $Cu(OH)_2$ diffraction peaks suggests that the produced Cu_2O nanoparticles are in their pure crystal phase.[39-40] Furthermore, the presence of the sharp diffraction peaks demonstrates that the prepared Cu_2O nanoparticles are highly crystalline.

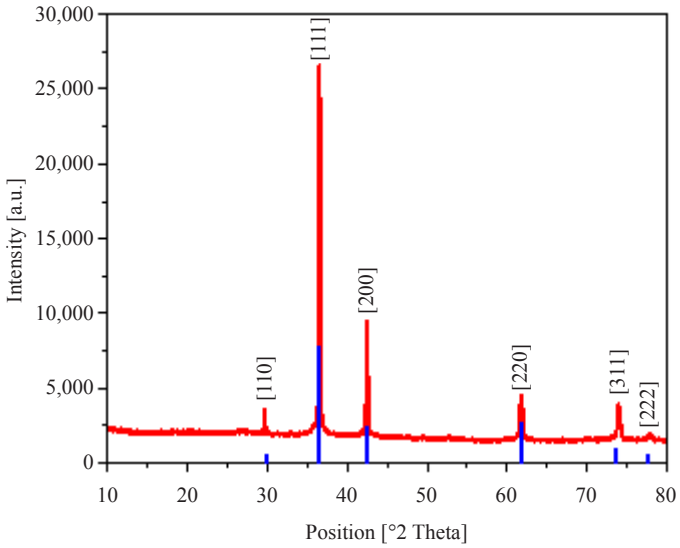

Figure 1. The XRD pattern of the prepared Cu_2O nanoparticles

Mainly, the particle size of Cu_2O depends on the synthesis mode, including initial concentration, surfactant content, stirring speed, etc. Meanwhile, the material particle shape depends on the above factors and the selected reducing agent. The SEM image of Cu_2O particles obtained by the reduction method with a mixture of glucose and ascorbic acid is shown in Figure 2. The morphology of the created Cu_2O has a uniform truncated block shape, similar to the research results of Yuanyuan Zhang's work.[42] Particle size distribution ranges from 50 nm to 150 nm, which is consistent with previous published works.[39-42]

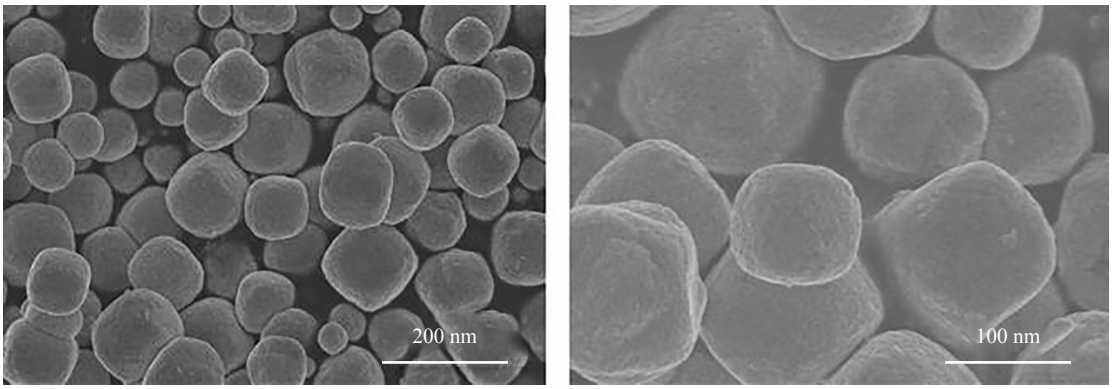

Figure 2. The SEM image of the prepared Cu_2O nanoparticles

The optical properties of the material were also evaluated through the UV-Vis DRS spectrum. The results presented in Figure 3 show that the band gap energy E_g of Cu_2O nanoparticles, calculated according to the formula of Tauc, is 1.945 eV, respectively, with the highest adsorption intensity at wavelength 477 nm. The results on the band gap energy of Cu_2O obtained are equivalent to previous publications.[28] Cu is a transition metal element. Although the outermost electron is distributed in the $4s^1$ layer, it belongs to the d subshell, so this single electron can easily change its energy level to achieve photocatalytic activity and is well represented in the visible region.[30]

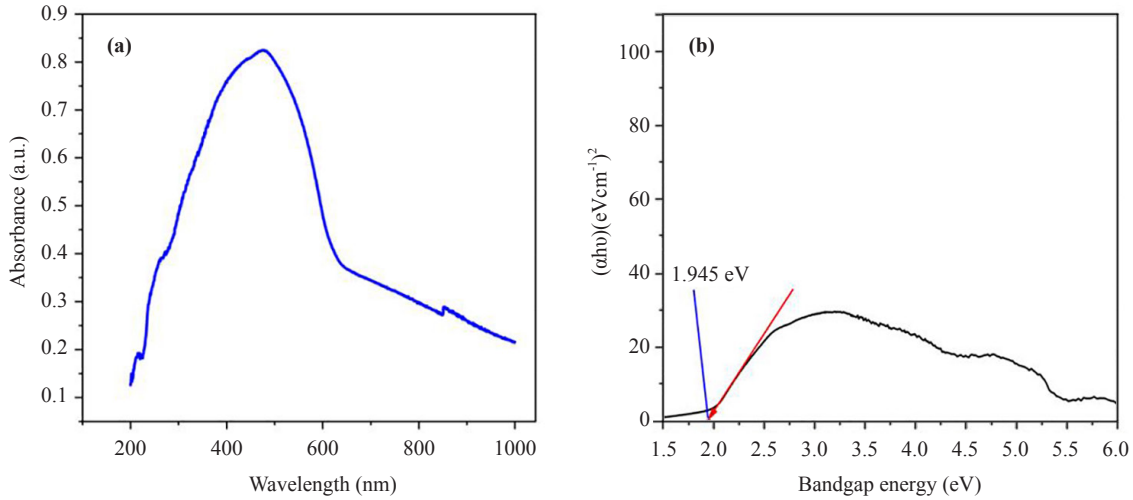

Figure 3. The UV-Vis DRS spectrum and band gap energy diagram of the prepared Cu_2O nanoparticles

3.2 *Removing methyl orange with Cu_2O photocatalyst*

The photocatalytic ability of nano Cu_2O to oxidize azo dye (methyl orange) was evaluated under simulated sunlight conditions. The result is shown in Figure 4. Experimental conditions were set up, including an initial MO concentration of 10 ppm, catalyst content of 0.5 g/L, and Xenon lamp power of 300 W. The results showed that MO rapidly degraded after 1 hour of irradiation and nearly lost color after 4 hours of exposure to light. Under simulated sunlight, electrons concentrated on the Cu_2O surface can theoretically react with adsorbed O_2 to produce $\cdot O_2^-$. After that, $\cdot O_2^-$ reacts with H_2O to produce hydrogen peroxide (H_2O_2) and hydroxyl radical ($\cdot OH$). This is the reason for the high activity of Cu_2O in decomposing MO. The prominent reaction modes of MO decomposition are $\cdot O_2^-$ and $\cdot OH$, and the photocatalytic mechanism of MO by Cu_2O is demonstrated through the reactions described as follows:[28-29]

$$hv + Cu_2O \rightarrow h^+ + e^-$$

$$O_2 + e^- \rightarrow \cdot O_2^-$$

$$\cdot O_2^- + 2H_2O \rightarrow 2 \cdot OH + H_2O_2$$

$$\cdot O_2^- + H_2O_2 \rightarrow \cdot OH + O_2 + OH^-$$

$$OH^- + h^+ \rightarrow \cdot OH$$

$$MO + \cdot O_2^- \left(\cdot OH\right) \rightarrow CO_2 + H_2O$$

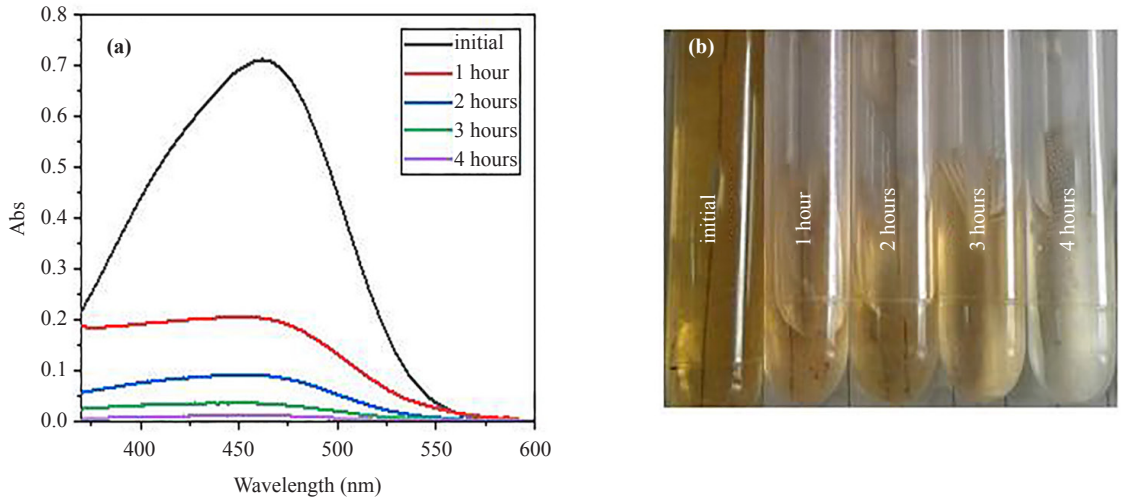

Figure 4. The UV-Vis spectrum (a) and digital image (b) of methyl orange with different illumination times

The photocatalytic activity of Cu_2O was tested for the decomposition of methyl orange under visible light irradiation for up to 4 hours. The MO decomposition efficiency of Cu_2O after 1, 2, 3, and 4 hours was 69.57, 84.88, 92.45, and 95.46%, respectively, as shown in the graph in Figure 5 (a). Compared to the MO decomposition efficiency under sunlight after 4 hours without any catalyst, it is 1.02%. The photocatalytic degradation data were calculated using a pseudo-first-order reaction kinetic model, as shown in Figure 5(b). The MO decomposition rate constant (k_1) of Cu_2O is 0.0127 min^{-1}.

Cu_2O was used six times to test the catalyst's recyclability in the MO decomposition reaction. This process was accomplished by centrifuging the photocatalyst, washing it in pure ethanol, and drying it in an oven at 80 °C for an hour. After using it in each subsequent round of catalytic reactions. According to the results, the response metabolism did not significantly change (Figure 6). It is obvious that the removal percentages of the MO decrease negatively after 5 cycles of testing, demonstrating that the Cu_2O nanoparticles photocatalyst is relatively stable in the aqueous solution.

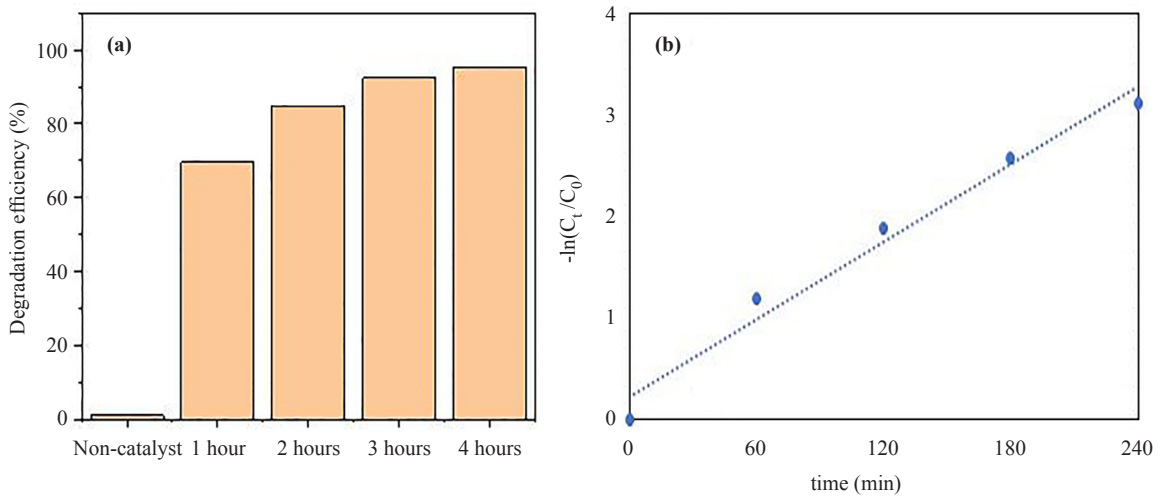

Figure 5. Degradation efficiency of methyl orange (a), and the pseudo-first-order kinetic of MO degradation (b) using Cu_2O photocatalyst under visible light irradiation

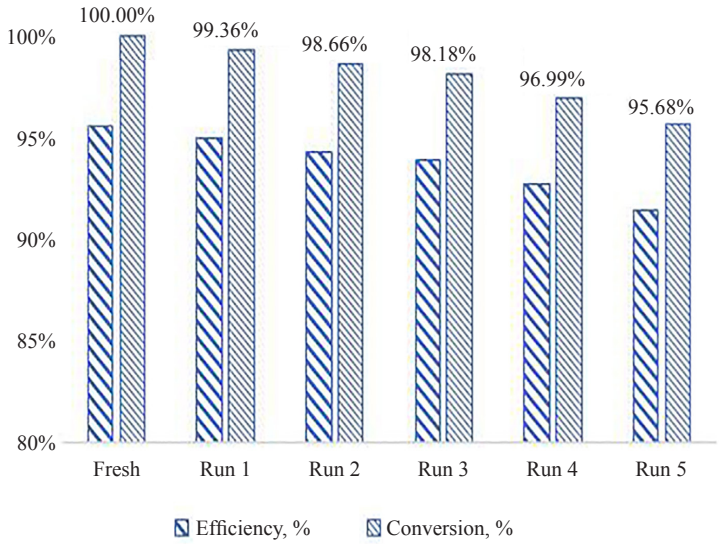

Figure 6. Reusability of nano Cu_2O photocatalyst for the removal of the MO dye

4. Conclusion

In summary, Cu_2O nanoparticles have been successfully fabricated using the reduction process with green reagents of glucose and ascorbic The obtained nano Cu_2O exhibited a consistently truncated block morphology, featuring particle sizes in the range of 50 to 150 nm. When subjected to visible light irradiation, the synthesized nano Cu_2O demonstrated noteworthy photocatalytic performance against methyl orange, achieving a removal efficiency of 95.46% after a 4-hour reaction period. According to our research, the Cu_2O photocatalyst has the potential to minimize environmental pollutants since it can effectively reduce methyl orange dye when exposed to visible light. The photocatalyst underwent negligible degradation during six cycles of recovery and repurposing. Cu_2O-based photocatalytic reduction is a potentially effective technique for reducing hazardous organic chemicals in general and azo compounds specifically.

Acknowledgments

This research is conducted and funded by the Department of Inorganic Materials, Institute of Chemistry and Materials.

Conflict of interest

The authors declare no competing financial interest.

References

[1] Barfi, B.; Asghari, A.; Rajabi, M.; Sabzalian, S. *J. Chromatogr. B Analyt. Technol. Biomed. Life Sci.* **2015,** *998-999*, 15-25.
[2] Barciela, P.; Perez-Vazquez, A.; Prieto, M. A. *Food Chem. Toxicol.* **2023,** *178*, 113935.
[3] Asif, M. F.; Bano, R.; Farooq, R.; Muhammad, S.; Mahmood, T.; Ayub, K.; Tabassum, S.; Gilani, M. A. *Dyes Pigm.* **2022,** *202*, 110284.
[4] Gester, R.; Torres, A.; Bistafa, C.; Araújo, R. S.; da Silva, T. A.; Manzoni, V. *Mater. Lett.* **2020,** *280*, 128535.
[5] Kantar, C.; Akal, H.; Kaya, B.; Islamoğlu, F.; Türk, M.; Şaşmaz, S. *J. Organomet. Chem.* **2015,** *783*, 28-39.
[6] Mughal, E. U.; Raja, Q. A.; Alzahrani, A. Y. A.; Naeem, N.; Sadiq, A.; Bozkurt, E. *Dyes Pigm.* **2023,** *220*, 111762.
[7] Haridevamuthu, B.; Murugan, R.; Seenivasan, B.; Meenatchi, R.; Pachaiappan, R.; Almutairi, B. O.; Arokiyaraj, S.; Arockiaraj, J. *J. Hazard. Mater.* **2024,** *461*, 132524.
[8] Sharma, J.; Sharma, S.; Soni, V. *Reg. Stud. Mar. Sci.* **2021,** *45*, 101802.
[9] Pay, R.; Sharrock, A. V.; Elder, R.; Mare, A.; Bracegirdle, J.; Torres, D.; Malone, N.; Vorster, J.; Kelly, L.; Ryan, A.; Josephy, P. D.; Allen-Vercoe, E.; Ackerley, D. F.; Keyzers, R. A. *Food Chem. Toxicol.* **2023,** *182*, 114193.
[10] Sevastre, A. S.; Baloi, C.; Alexandru, O.; Tataranu, L. G.; Popescu, O. S.; Dricu, A. *Saudi J. Biol. Sci.* **2023,** *30*, 103599.
[11] Kokturk, M.; Altindag, F.; Ozhan, G.; Calimli, M. H.; Nas, M. S. *Comp. Biochem. Physiol. C Toxicol. Pharmacol.* **2021,** *242*, 108947.
[12] Birniwa, A. H.; Ali, U.; Jahun, B. M.; Saleh Al-dhawi, B. N.; Jagaba, A. H. *Case Stud. Chem. Environ. Eng.* **2024,** *9*, 100553.
[13] Guo, T. S.; Yang, S. D.; Cui, H. M.; Yu, Q. F.; Li, M. F. *Int. J. Biol. Macromol.* **2023,** *253*, 127012.
[14] Boushara, R. S. H.; Johari, K.; Mustafa, N. M. *Mater. Today: Proc.* **2024,** *97*, 30-35.
[15] Leng, Q.; Xu, S.; Wu, X.; Wang, S.; Jin, D.; Wang, P.; Wu, D.; Dong, F. *Environ. Res.* **2022,** *214*, 114064.
[16] Liu, X.; Chen, Z.; Du, W.; Liu, P.; Zhang, L.; Shi, F. *J. Environ. Manage.* **2022,** *311*, 114775.
[17] Teguia Doumbi, R.; Noumi, G. B.; Domga. *Case Stud. Chem. Environ. Eng.* **2021,** *3*, 100068.
[18] Zafar, S.; Bukhari, D. A.; Rehman, A. *Saudi J. Biol. Sci.* **2022,** *29*, 103437.
[19] Tizazu, S.; Tesfaye, G.; Wang, A.; Guadie, A.; Andualem, B. *Heliyon* **2023,** *9*, e16857.
[20] Tu, J.; Lu, C.; Chen, Z.; Zhang, Q.; Song, Y.; Li, H.; Han, Y.; Hou, Y.; Guo, J. *Int. Biodeterior. Biodegrad.* **2022,** *170*, 105401.
[21] Karimi, F.; Zare, N.; Jahanshahi, R.; Arabpoor, Z.; Ayati, A.; Krivoshapkin, P.; Darabi, R.; Dragoi, E. N.; Raja, G. G.; Fakhari, F.; Karimi-Maleh, H. *Environ. Res.* **2023,** *238*, 117202.
[22] Bao, L. L.; Li, Y.; Xi, Z.; Wang, X. Y.; Afzal, M.; Alarifi, A.; Srivastava, D.; Prakash, O.; Kumar, A.; Jin, J. C. *J. Mol. Struct.* **2023,** *1292*, 136103.
[23] Onwudiwe, D. C.; Nkwe, V. M.; Olatunde, O. C.; Ferjani, H. *Ceram. Int.* **2023,** *49*, 19451-19462.
[24] Zhan, X.; Ding, C.; Chen, B.; Fang, Y. *Opt. Mater.* **2024,** *147*, 114725.
[25] Hering, K. P.; Brandt, R. E.; Kramm, B.; Buonassisi, T.; Meyer, B. K. *Energy Procedia* **2014,** *44*, 32-36.
[26] Yang, F.; Peng, W.; Zhou, Y.; Li, R.; Xiang, G.; Yue, J. Z.; Zhang, J.; Zhao, Y.; Wang, H. *Vacuum.* **2022,** *198*, 110876.
[27] Zhang, D.; Yang, J.; Wang, J.; Yang, J.; Qiao, G. *Opt. Mater.* **2020,** *100*, 109612.
[28] Moghanlou, A. O.; Bezaatpour, A.; Sadr, M. H.; Yosefi, M.; Salimi, F. *Mater. Sci. Semicond. Process.* **2021,** *130*, 105838.
[29] Liaqat, M.; Iqbal, T.; Maryam, I.; Riaz, K. N.; Afsheen, S.; Sohaib, M.; Al-Zaqri, N.; Warad, I.; Al-Fatesh, A. S. *J.*

Photochem. Photobiol. A: Chem. **2024,** *446*, 115122.
[30] Ying, T.; Liu, W.; Yang, L.; Zhang, S.; Wu, Z.; Li, J.; Song, R.; Dai, W.; Zou, J.; Luo, S. *Sep. Purif. Technol.* **2024,** *330*, 125272.
[31] Thi, L. N.; Tuyet, M. N. T.; Minh, H. D. T.; Thu, H. T. T.; Kim, N. N.; Xuan, A. T.; Ngoc, D. T.; Dang, C. H.; Cong, T. N.; Lan, A. L. T. *Vietnam J. Catal. Adsorpt.* **2021,** *10*, 65-70.
[32] Anh Thư, N. T.; Mỹ Linh, N. L.; Đức, H. V. *Hue Univ. J. Sci. Nat. Sci.* **2020,** *129*, 43-48.
[33] Li, N.; Hu, J.; Li, J.; Cheng, M.; Wei, T.; Liu, Q.; Wang, R.; Li, W.; Ling, Y.; Zhang, Y.; Liu, B. *J. Alloys Compd.* **2024,** *976*, 173074.
[34] Wang, N.; Tao, W.; Gong, X.; Zhao, L.; Wang, T.; Zhao, L.; Liu, F.; Liu, X.; Sun, P.; Lu, G. *Sens. Actuators B: Chem.* **2022,** *362*, 131803.
[35] Huang, C. Y.; He, X. R.; Jhang, J. J.; Wu, J.-H.; Wu, T. H.; Lin, T.-H. *Sens. Actuators A: Phys.* **2022,** *347*, 113992.
[36] Lakshmanan, A.; Alex, Z. C.; Meher, S. R. *Mater. Sci. Semicond. Process.* **2022,** *148*, 106818.
[37] Sun, B.; Chen, H.; Yan, K.; Feng, X.-D. *Opt. Mater.* **2022,** *131*, 112642.
[38] Enebe, G. C.; Lukong, V. T.; Mouchou, R. T.; Ukoba, K. O. *Mater. Today: Proc.* **2022,** *62*, S145-S150.
[39] Okoye, P. C.; Azi, S. O.; Qahtan, T. F.; Owolabi, T. O.; Saleh, T. A. *Mater. Today Chem.* **2023,** *30*, 101513.
[40] Cuatto, G.; Zoli, M.; Gallone, M.; Guzmán, H.; Castellino, M.; Hernández, S. *Chem. Eng. Res. Des.* **2023,** *199*, 384-398.
[41] Gonçalves, C. B.; da Silva, R. T.; Dalenogare, G.; Gonzaga, I. M. D.; Mascaro, L. H.; Ferrer, M. M.; Assis, M.; Longo, E.; de Carvalho, H. B. *Surf. Interfaces* **2023,** *42*, 103397.
[42] Zhang, Y.; Zhang, Z.; Zhang, Y.; Li, Y.; Yuan, Y. *J. Colloid Interface Sci.* **2023,** *651*, 117-127.